A Century of Tidal Variability in the North Pacific Extracted from Hourly Geomagnetic Observatory Measurements at Honolulu

Robert H. Tyler[1,2]

[1]NASA Goddard Spaceflight Center
[2]Joint Center for Earth Systems Technology, University of Maryland Baltimore County

Key Points:

- Analyses of geomagnetic data at Honolulu shows modulation in the tides consistent with that seen in tide-gauge data.
- The tidal magnetic modulations appear to be due to ocean and not ionospheric tides.
- If confirmed, this study establishes the opportunity for using historical geomagnetic records in physical oceanography.

Corresponding author: Robert H. Tyler, NASA Goddard Spaceflight Center, Geodesy and Geophysics Laboratory Code 61A, Greenbelt MD, 20771

Abstract

Previous analyses of hourly tide-gauge data taken at Honolulu since 1905 have shown that both sea level and the amplitude of the tides have increased synchronously over time, and a process has been proposed whereby the common cause is an increase in ocean temperature. Validation with independent data of this change in tides, as well as the proposed cause, has been lacking. Ocean tides also generate magnetic fields that reach far outside the ocean, and tidal signals are clearly seen in the hourly data since 1905 from the Honolulu geomagnetic observatory. Here, it is found that the tidal amplitudes have increased synchronously in the tide-gauge and magnetic records, providing independent support for the previous results. Further information about the changing ocean is likely contained in the historical data from geomagnetic observatories as well as the global coverage of modern satellite magnetic surveys.

Plain Language Summary

In previous work, it has been shown that tidal amplitudes as recorded by tide-gauge data at Honolulu show interannual modulations as well as a century long trend toward larger amplitudes. It was proposed that (1) these changes in the tidal amplitudes are indeed reflective of changes in important ocean parameters (rather than uninteresting local effects) and (2) that the increase is indirectly due to increasing ocean temperature. Ocean tides also generate magnetic fields and the long record from the Honolulu geomagnetic observatory provides an opportunity for validation using an independent data set. Here, results for the modulation and trend are supported by the magnetic data and are also consistent with the explanation regarding ocean warming".

1 Goal and Approach

Tides in the ocean are forced by the differential gravitational pull of the Moon and of the Sun. While the Sun is more massive, it is also further away. The result is that the forces by the Moon are typically about twice as large as that of the Sun. In either case, these forces vary in time with the celestial positions of these bodies and can be described with very high accuracy even for times a century past.

The tidal response of the ocean depends, however, not just on the forces but also on variability in its own internal parameters. If these parameters were invariant, then (after accounting for the time variations in the forces) one would expect invariance in the tidal-response amplitudes. Oceanographers have, however, observed that in most long records of tide-gauge data these tidal amplitudes are not constant, and in some cases the observed modulations appear to reflect real changes in the ocean's tidal response over time (Mitchum & Chiswell, 2000; Colosi & Munk, 2006; Ray, 2006, 2009; Müller et al., 2011; Devlin, Jay, Zaron, et al., 2017; Ray & Talke, 2019; Devlin, Jay, Talke, et al., 2017; Haigh et al., 2020; Talke & Jay, 2020). It is both expected and demonstrated that the tidal amplitudes observed by a coastal tide gauge can be affected locally by both anthropogenic projects (e.g. dredging) and natural processes that have little to do with larger-scale changes in the ocean. Potential significance to ocean and climate studies has arrived, however, from observations of correlated trends and modulations between geographically separated tide gauge data, and cases where the tidal modulations are seen to correlate with changes in the observed sea-level height.

Long tide-gauge records from Honolulu and Hilo, Hawaii are remarkable in demonstrating both of these types of correlations (Mitchum & Chiswell, 2000; Colosi & Munk, 2006). It has been proposed that the correlations in these long records may reflect changes in ocean temperature and stratification over the last century (Colosi & Munk, 2006), but elements of this proposal have been difficult to further test because of limitations in observational coverage from independent data that extend back that far. The goal of this paper is to introduce the use of geomagnetic records in addressing past ocean variability, and to show that the specific

questions regarding tidal variability at Hawaii can be addressed with the long records from the Honolulu geomagnetic observatory.

The approach here is to calculate and compare the tidal modulations seen in the geomagnetic data with the tidal modulations seen in the sea-surface (tide-gauge) data. Here, sea-surface tidal modulations are extracted using a longer time series and different method than in the previous studies. The results confirm the modulations previously described and therefore, independent of the geomagnetic component of this study, also provide confirmation and temporal extension of the previous work. Importantly, the new method for extracting the modulations is also well suited for exploiting the vector nature of the magnetic data and for differentiating oceanic versus ionospheric tidal components.

2 Sea-Surface Tides at Honolulu

Tide-gauge records at Honolulu are immediately remarkable because of their long, nearly continuous coverage. While records extend back to 1872, good hourly data begin only in 1905 and extend, in this study, to 2017. In (Mitchum & Chiswell, 2000; Colosi & Munk, 2006), the tide-gauge series between 1915-2000 was considered and the method of complex demodulation was used to extract the tidal modulations at a prescribed M_2 lunar semi-diurnal periodicity. The results revealed that the tidal amplitude and phase have shown inter-annual variations as well as a long-term increase. Further, these modulations in the tides were shown to be correlated with the slowly changing mean sea level.

Why should the amplitude of the high-frequency tides vary together with the slow variations in mean sea level? An explanation has been proposed (Mitchum & Chiswell, 2000; Colosi & Munk, 2006) whereby the mean sea level is expected to be correlated with a mean depression of the thermocline separating warm surface water from deeper, cooler water; Aside from the familiar “external” tides, in a stratified ocean there are also “internal” tides that have a small manifestation in the sea-surface displacement. Changes in the stratification (or thermocline depth) affect the production and propagation of internal tides. Changes over time in the stratification have altered the propagation speed of the internal waves and thereby the degree to which their surface manifestation combines constructively (or destructively) with the external tide to produce the tidal amplitude measured by the tide gauge. While the observed modulations of the tide may reflect changes in ocean stratification due to multiple causes, the long-term increase in tidal amplitude over the last century is attributed to the warming of the surface ocean.

In (Mitchum & Chiswell, 2000; Colosi & Munk, 2006), the tidal modulations in the Honolulu tide-gauge data were extracted using complex-demodulation. As in the design of amplitude-modulation (AM) radio, complex demodulation involves the prescription of a carrier wave that is modulated by the lower-frequency signal of interest. The carrier signal used in (Mitchum & Chiswell, 2000) was sinusoidal with the M_2 lunar frequency, which has a period of 12.42 hours corresponding with a frequency that is twice the mean rate at which the Moon traverses westward over lines of the spinning Earth’s longitude. In (Colosi & Munk, 2006), the carrier wave used was the tidal potential. In both cases, the waveform is being prescribed a priori rather than discovered empirically from the data.

The approach used in this study does not require prescription of a carrier wave. First, the lunar longitudinal position (referred to here as simply “lunar azimuth”) is not approximated from the constant M_2 frequency but is instead taken from the precise astronomical location (ephemeris) of the Moon with respect to Earth. Second, the waveform (describing the shape of the oscillation over a tidal cycle) is obtained empirically from the data, rather than being prescribed a priori. This is important in interpreting the magnetic data because ocean tidal signals should have near-sinusoidal waveforms dependent on the lunar azimuth, whereas the competing ionospheric lunar magnetic signals depend on solar-radiation affecting the ionospheric conductivity and therefore have more complex luni-solar waveforms.

In the method of this study (see Section 6) the tide gauge hourly series is first whitened by taking the time derivative, and the result is then detrended. This hourly data reflects sampling every 15 degrees of mean rotation of the Earth with respect to the sun. The data is interpolated onto 'hourly' points reflecting instead 15 degrees of rotation with respect to the Moon. The time series data is then reshaped into a lunar azimuth-vs.-time data matrix and the data is smoothed with respect to time. The smoothing removes or reduces signals not phase locked with the lunar orbit.

The result is shown in Fig. 1. A very clear semidiurnal waveform is seen, as expected. Also apparent are striations due to missing data as well as abrupt phase shifts due to baseline adjustments of the tide-gauge observatory. A century-long trend toward increasing amplitudes in the semidiurnal waveform is also apparent, as well as inter-annual variations. Other features (e.g. diurnal tides) are likely to be present but cannot be discerned visually. The amplitude of the waveform is about 2000 mm/day. The approximate amplitude of the wave sea-surface height can be obtained by dividing by the lunar semidiurnal frequency ($\sim$ 12.1 radians/day), giving a wave amplitude of about 170 mm.

To extract further information from this data matrix, singular-value decomposition is used to find the empirical orthogonal functions (EOFs , also called "principal components"), and the results are also shown in Fig. 1. The waveforms for the first 4 EOFs are shown together with their associated time series. Each EOF mode is described by its waveform modulated by its time series. The bar graph shows that nearly all of the variance in the data is explained by the first EOF. EOF 1 has a clear lunar semi-diurnal waveform, as expected, and its time series shows an upward trend as well as inter-annual variations. The next most important mode, EOF 2, is seen to also have a semi-diurnal waveform, though out of phase with EOF 1. Looking at its time series, it is clear that EOF 2 is simply providing a correction for the baseline shifts. Therefore, the time series describing the root-mean-square amplitude of the lunar semi-diurnal tide shall be taken to be the root sum of squares of the EOF 1 and EOF 2 components. EOF 3 describes a diurnal tide waveform with no clear secular trend. EOF 4 shows a more complex diurnal/quarter-diurnal waveform, also with no clear trend.

3 Geomagnetic Tides at Honolulu

Global ocean tides generate magnetic fields that reach far outside the ocean (Tyler et al., 2003; Sabaka et al., 2015, 2016, 2018; Grayver & Olsen, 2019; Sabaka et al., 2020), and tidal signals are clearly seen in the hourly data since 1905 from the Honolulu geomagnetic observatory (Love & Rigler, 2014).

For this study, detrended time-differenced hourly records from 1905-2017 are examined. The magnetic vector records in fact include three time series, referred to here as E, N, R, associated with the eastward, northward, and radial vector components. In the analysis here, the vector data has been rotated into new components E^*, N^*, R^*. A singular-value decomposition was performed to determine the statistical axes of variability such that the nominal components E^*, N^*, R^* are then aligned with these axes and represent, in this order, axes of decreasing variability. It is found that R^* remains close to representing the radial component R. The reason for rotating the geomagnetic vector is to produce a component R^* that is expected to be influenced less by magnetic fields generated by large-scale electric currents in the upper atmosphere. In the approximation that these currents flow as a horizontal sheet above Honolulu, their direct influence on R is zero. The replacement of R with R^* is an objective approach in selecting the geomagnetic vector component with the highest expected ocean-tidal signal-to-noise ratio.

A data matrix and EOF analysis identical to that performed above for the sea-surface data is applied to R^* and the results, shown in Fig. 2, have many elements in common with the sea-surface results. Visually apparent in the smoothed magnetic data is a lunar semi-diurnal waveform as well as observatory baseline shifts, inter-annual variability and a trend.

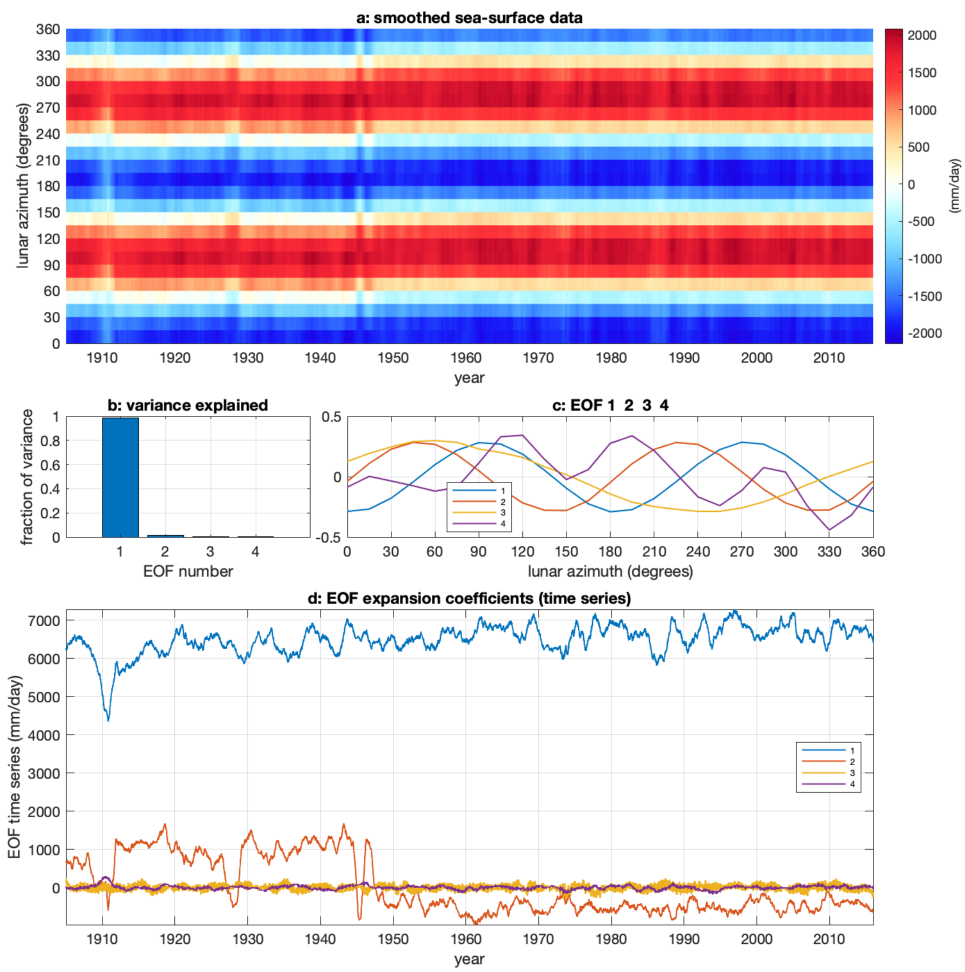

Figure 1. Smoothed sea-surface data at Honolulu is shown as a function of year and lunar azimuth (a). An EOF analysis reveals that 99 percent of the variance in this data can be described by the first EOF (b), describing a semi-diurnal wave form (c), with EOF 2 providing a correction for observatory baseline shifts (c, d). The EOF 1 time series shows inter-annual variations as well as an upward trend toward increased tidal wave amplitudes over the century (d).

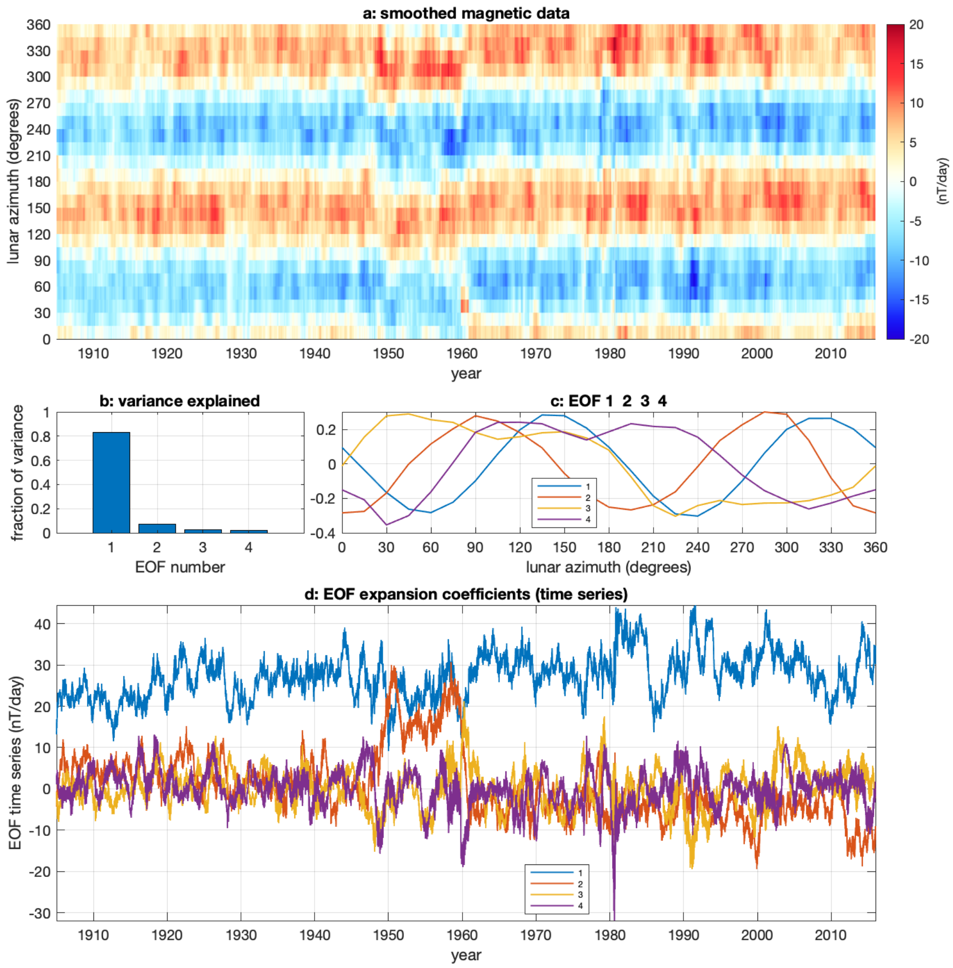

Figure 2. Smoothed geomagnetic data at Honolulu is shown as a function of year and lunar azimuth (a). An EOF analysis reveals that 83 percent of the variance in this data can be described by the first EOF (b), describing a semi-diurnal wave form, with EOF 2 providing a correction for observatory baseline shifts (c, d). The EOF 1 time series shows inter-annual variations as well as an upward trend toward increased tidal wave amplitudes over the century (d).

The lunar semidiurnal wave amplitudes (obtained by dividing by 12.1) are about 1.25 nT. It is also apparent that the lunar-tidal signal-to-noise ratio in the geomagnetic data is much lower than in the sea-level data.

EOF 1 explains 83 percent of the variance and EOF 2 explain 8 percent. Both EOF 1 and EOF 2 show waveforms that are nearly semi-diurnal. The waveforms for EOFs 3 and 4 have a complex shape with a strong diurnal component. The EOF time series show, as with the sea-surface data, that EOF 2 is primarily providing a correction to the observatory baseline shifts (due in this case to observatory re-location) and therefore, the time series describing the root-mean-square amplitude of the lunar semi-diurnal tide shall be taken to be the root sum of squares of the EOF 1 and EOF 2 components.

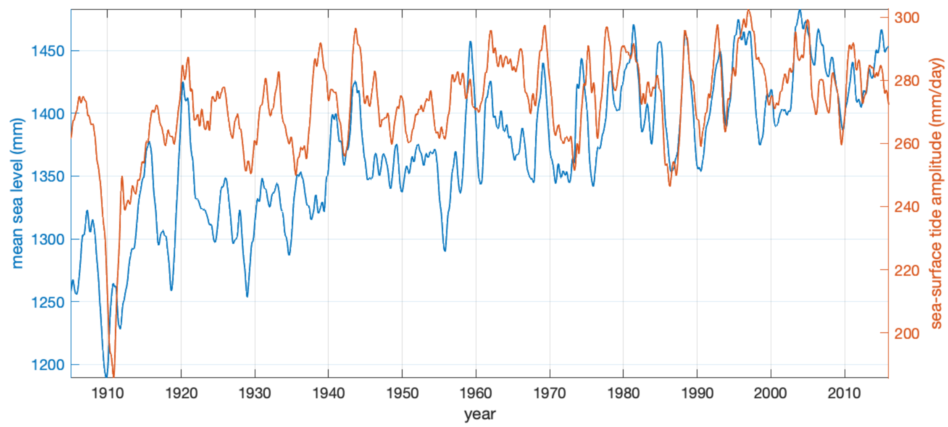

Figure 3. The tidal amplitude in the sea-surface data is found to be significantly correlated with the slowly varying mean sea level. The correlation coefficient (0.702) is above the 95 percent confidence level (0.636). The detrended series also remain correlated (0.581) above the 95 percent level (0.342).

4 Trends and correlations

Having isolated time series describing the modulation of the tidal amplitudes in both the sea-surface and geomagnetic data, here trends and correlations between the series are examined.

In Fig. 3, the low-passed mean sea level is shown together with the tidal amplitude in the sea-level data. The Pearson correlation coefficient is 0.702 (0.581 for the detrended series). To avoid over-estimation of the significance, the significance reference levels have been calculated using the method of (Sciremammano, 1979) designed for serially correlated data (i.e. data that has fewer effective degrees of freedom than data points). These correlation coefficients, 0.702/0.581, are both above the 95 percent significance levels (0.636/0.342). This indicates that the two series are significantly correlated both in the trend and interannual variability.

In Fig. 4, the geomagnetic tidal amplitude is shown together with the sea-surface tidal amplitude. The correlation coefficient is 0.453/0.292 for the raw/detrended series. The correlation is above the 95 percent significance level (0.450) for the raw data, while for the detrended data, the correlation is above the 90 percent level (0.257) and below the 95 percent level (0.346). It appears that the geomagnetic R^* series is significantly correlated with the sea-surface data both in trend and inter-annual variability. By contrast, the analysis using instead the E^* or N^* geomagnetic components shows no similar trend nor significant correlations with the sea-level tide data. As there are 24 EOF time series for each of the three components, the significant correlation described can be compared to 70 other correlations where significance was not found nor expected.

5 Discussion and Conclusions

The primary results of this study have two parts. First, by using a qualitatively different method of demodulation with fewer a priori assumptions, as well as a time series 27 years longer, the study has provided validation and extension to previous results showing a correlation between semi-diurnal lunar tidal amplitudes in sea-surface data at Honolulu and the slowly varying mean sea level over more than a century. Second, the modulations and trend

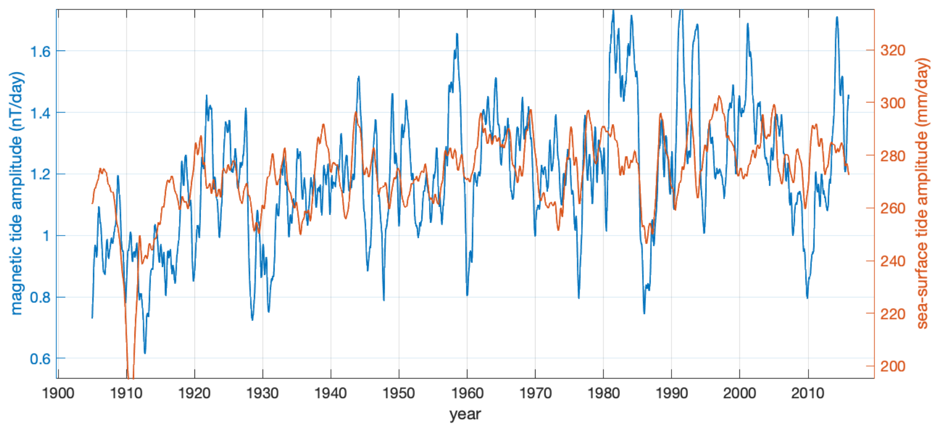

Figure 4. The tidal amplitudes in the sea-surface and geomagnetic data are found to be significantly correlated. The correlation coefficient (0.453) is above the 90 percent confidence level (0.450). The correlation coefficient of the detrended series (0.292) is between the 90 percent (0.257) and 95 percent (0.334) significance levels.

in the sea-level tidal amplitudes are shown to be supported by similar variations in the tidal magnetic fields seen in the independent geomagnetic data.

This introduction of geomagnetic data into physical oceanography needs to be carefully examined because of the important opportunity for harvesting oceanographic information contained in the vast collection of land and satellite magnetic observatory data, and because of the challenges in separating and interpreting the relatively small oceanic magnetic components. Immediate intuition toward this challenge can be seen by comparing Figs. 1a, 2a; whereas the ocean tides are a dominant contributor to the sea-surface data, the tidal signal in the magnetic data may suffer contamination by other sources. In this application, contamination may come from the broader-band cusps associated with the strong and nearby solar semi-diurnal frequency processes as well as the magnetic fields due to ionospheric tides. These competing signals do not have the sinusoidal waveforms of ocean tides but rather a more complex structure including a square-wave like dependence on solar radiation. The EOF demodulation approach with its empirically obtained waveforms is aimed at leveraging this distinction. When, for example, the same analyses as conducted here are performed using the solar rather than lunar azimuth, the leading EOF for the sea-surface data shows an expected near-sinusoidal variation clearly due to the ocean tides driven by solar gravity, whereas the magnetic data shows a waveform reflecting instead solar radiation (an expected solar-quiet waveform modulated by a time series well correlated with the sunspot history), thereby demonstrating that the solar tidal magnetic signal is not predominantly oceanic.

Further work on this topic could include the following. First, aside from distinguishing oceanic versus atmospheric tidal signals in the magnetic data, the EOF demodulation approach might be further applied to the sea-level data to determine if the small departures of the empirical waveforms from sinusoidal can be used to test proposed processes involving nonlinear barotropic + baroclinic tides. Second, the potential influence of ionospheric lunar tides should be further examined. The lunar tidal contribution of ionospheric magnetic fields has been described in (Schnepf et al., 2018). At Honolulu, the model data gives a vertical amplitude of 0.094 nT, compared to 1.25 nT found here for R^*. As an additional check for ionospheric influence, two other methods of demodulating R^* were conducted (complex demodulation using the sine/cosine of twice the lunar azimuth as a carrier wave; and robust linear fitted coefficients each year) and showed similar magnetic modulations as seen in Fig. 4, whereas

demodulation using as the carrier wave the Chapman phase law lunisolar components (a harmonic series that tries to represent the square-wave like solar influence in representing the ionospheric lunar tidal signals) showed no similar trend or modulation as in Fig. 4. A preliminary conclusion is that R^* reflects oceanic rather than ionospheric tidal processes. Improved models of the ionospheric tides with better validation of the associated magnetic fields would be very helpful.

Finally, better models of the fluid and electrodynamic ocean tidal processes would be very helpful in identifying which component of the ocean tides have changed. Such models do not yet exist and require development and possibly more observations before they can be constructed. The ideal use of the model would be as in (Tyler et al., 2003) where flow from a global barotropic tidal model was used to drive an electrodynamic model to predict the global magnetic fields due to the M_2 tides. This forward-model prediction motivated the extraction of an M_2 map from satellite magnetic data. The forward-model map was independent/blind of the observational map as it was produced in advance. The production of the observational map could refer to the model prediction as a check but was otherwise independent. The remarkable agreement between the two independent maps provided then cross-validation for both the forward and observational models and an impliit description of the underlying processes. The extension of this approach to this regional-domain, high-resolution Hawaiian application involving internal tides is not immediate. Only partial descriptions of the internal tide field are available (Zhao et al., 2011; Zhao, 2016) and even the highest-resolution conductivity climatology data (Reagan et al., 2020) may be inadequate. It seems that an alternative approach of first fitting satellite magnetic data to a regional model and letting the observed magnetic field distribution guide forward model development might be more appropriate.

Returning to the conclusions from this initial study, neither the sea-surface nor magnetic tidal modulation time series can uniquely indicate which components of the tides have changed to bring about the modulation. But some possibilities can be described. Combined with other evidence, the sea-surface modulation is thought to ultimately be the consequence of warmer surface waters (Mitchum & Chiswell, 2000; Colosi & Munk, 2006). Warmer surface waters would increase the conductivity, thereby increasing the strength of non-local electric currents that are driven by large-scale tides and forced to flow over the Hawaiian Ridge and around the islands. Because of the increased conductivity (decreased resistance), the strength of the electric currents and associated magnetic fields near the ridge would increase with ocean warming but also (more locally, presumably) with the depressed-thermocline phase of an internal tide. Both of these processes would explain why the surface and magnetic tidal amplitudes increase together, and they are generally consistent with the process proposed in (Mitchum & Chiswell, 2000; Colosi & Munk, 2006). Another possibility is that the magnetic field modulation is due to the magnetic field generated by the local external or internal tide which has changed over time. Finally, the ocean surface forces upward propagating waves that contribute to the ionospheric tide and so potential links between the ocean and ionospheric tides must continue to be considered until they can be more carefully ruled out.

Much further study is warranted on this topic as the magnetic data provides an important opportunity not only for validation using an independent data set but also to isolate which tidal elements have changed. The sea-surface and magnetic fields are generated by the tides in different ways and therefore modulations seen in both provide a constraint on which changing tidal processes could be responsible. The time-series analyses described in this initial study are aimed at demonstrating the correlations using the fewest number of processing steps and applying these steps identically to both data sets. Additional justifiable processing steps (e.g. selecting magnetic data to avoid magnetic storms or daytime, spectral-filtering and removing of solar model signals) can improve the correlation coefficients but raise then questions as to the dependence of the reported coefficients on these optional choices. The approach here is intended to provide a starting point for analyses that can be immediately extended to other locations as well.

6 Methods

6.1 Data and Pre-processing

All data used is publicly available (see Data Availability section). The time axis on which the emphemerides were calculated coincides with the hourly axes of the magnetic data but includes a rate three times higher such that each time step corresponds to 5 degrees of the Moon's mean motion westward as seen from Earth. The azimuth ϕ is the monotonically increasing (i.e. unwrapped $\phi = 0, 5, 10...360, 365, 370...$) westward longitude of the Moon as seen from the fixed-Earth frame and with respect to the prime meridian. The raw data used then consists of five time series: sea level at Honolulu, the three geomagnetic components from the Honolulu geomagnetic observatory, and lunar azimuth.

As with many geophysical series, the sea-level and geomagnetic data have red spectra with more energy at lower frequencies. To pre-whiten the series as well as reduce the influence of baseline shifts, the series (all but lunar azimuth) were time differenced and the result detrended. A centered finite-difference method was used for the time-differencing. No interpolation to fill missing data was done as regularly spaced data is not required for the EOF analysis. Instead of using all three geomagnetic series, the vector data was first rotated (using a singular-value decomposition just as in the EOF analysis described below) and only an R^* component was selected. The R^* component is the third mode and therefore is the axis of least variability. It is also primarily radial (i.e. aligned with R); the empirically-found rotation can be written as $R^* = 0.3967E - 1.492N + 0.9057R$.

A common time axis for all data was chosen to be the times associated with lunar azimuth at regular 15-degree intervals. These 15-degree steps are a little longer than 1 hour (because it takes the Earth about 24.8 hours to rotate with respect to the Moon) and also not constant because there is a small variability in the rate of the Moon's orbital progression. Hence, the common time axis is regularly spaced not in time but instead in lunar azimuth. The data series were interpolated onto this common time axis.

6.2 Analysis

Next, data matrices are formed by sequentially wrapping/reshaping the series through the the 24 lunar azimuth points. The result is a data matrix of 24 columns, each column describing a time series associated with data values when the Moon is at a specific azimuth. The mean for each row is removed. This data matrix is then smoothed with a low-pass moving mean filter with window approximately one year. The smoothed data matrices, rotated by 90 degrees counter-clockwise and shown in the upper frames of Figure 1 and 2, provide a description of the slowly-changing dependence of the data on lunar azimuth and time. The smoothing tends to filter out signals not phase locked with the lunar azimuth.

The Empirical Orthogonal Function (EOF) analysis uses singular-value decomposition to find all 24 eigenfunctions of the covariance matrix of the smoothed data matrix.

The tidal amplitude series in Figs. 3, 4 were obtained by taking the root sum of squares of EOF 1 and EOF 2 and then filtering using a low-pass moving mean filter with a window of about 90 days (approximate because the series are regularly sampled in azimuth rather than time).

To estimate the potential contribution to R^* of the lunar ionospheric tidal geomagnetic field, the model data in (Schnepf et al., 2018) was obtained and the value for the radial magnetic component was interpolated onto the location of the geomagnetic observatory. While the radial component is weak (0.094 nT), the eastward (1.0 nT) and northward (0.08 nT) are stronger and approach the 1.25 nT strength of R^*. While this provides provisional confirmation that oceanic rather than ionospheric tides dominate in R^*, further validation of the ionospheric tidal magnetic model is required.

The generation of the ocean tidal magnetic fields depend on both the strength and gradients of the radial component of the main geomagnetic field. The effects on the strength were estimated by replacing R^* with R^* divided by the Honolulu observatory radial geomagnetic component and reconducting the analyses. The results were similar. While the correlation coefficient between the geomagnetic and sea-level tidal modulations increased from 0.45 to 0.50, the recalculated confidence levels also changed and the significance level remained about the same.

It is appreciated that the correlation coefficient between two series means very little without a description of the number of degrees of freedom in the data set. This can be demonstrated by showing that the correlation coefficients discussed can all increase remarkably by simply first applying a low-pass filter to the series. This does not mean that the correlations become more significant; the filtering also decreases the effective degrees of freedom by increasing the serial correlation in each series. In this paper correlations have been claimed as "significant" only where the correlation coefficients exceed significance levels calculated from the data itself using the method in (Sciremammano, 1979) designed for compensating for serial correlation. Support for the significance of the correlations in the tidal modulations between the sea-surface and geomagnetic series was also obtained by finding that the sea-level modulations were not significantly correlated with any of the 22 higher (EOF > 2) series in R^* nor any of the 48 EOF series in E^* and R^*. Hence, in these other 70 time series there have been 70 opportunities for a spuriously significant correlation, but none were found. It is also important that the significant correlation found (involving EOF 1 and 2) is also associated with an empirically derived lunar-semidiurnal waveform, as expected for the ocean tides, whereas none of the other EOFs of R^* showed this waveform.

Finally, it was found that data selection can improve (or reduce) the correlations. By selecting from the magnetic data only night-time, solar-quiet, or other data distributions, the competing solar effects are reduced, but so is the number of degrees of freedom in the resulting series such that an improvement in the resulting significance levels is not systematic. Because there are many different choices for data selection, increasing the opportunity for reporting a spuriously significant correlation, the study here has reported only the case where all data was used (as also used in (Love & Rigler, 2014)). Interestingly, the 1905-1915 section of surface-tide modulation was omitted in (Colosi & Munk, 2006) as it was regarding as not appearing realistic; a strange dip can be seen in Fig 1. A similarly strange dip, however, is also seen in R^*, and therefore the omission of this section did not seem justified for this study and the data was retained.

6.3 Data Availability

The Honolulu sea-surface data was obtained from the University of Hawaii Sea Level Center (the "research quality" series was downloaded from http://uhslc.soest.hawaii.edu/data/?fd). The Honolulu geomagnetic-observatory data was obtained from the World Data Center (WDC) for Geomagnetism at Edinburgh (http://www.wdc.bgs.ac.uk). The lunar "azimuth" was calculated at the times in the past from Cartesian ephemerides for the Moon obtained using the SPICE Toolkit (https://naif.jpl.nasa.gov/naif/toolkit.html) with the 'IAU_EARTH' frame kernel.

References

Colosi, J. A., & Munk, W. (2006). Tales of the Venerable Honolulu Tide Gauge. *Journal of Physical Oceanography*, *36*(6), 967–996.

Devlin, A. T., Jay, D. A., Talke, S. A., Zaron, E. D., Pan, J., & Lin, H. (2017). *Coupling of sea level and tidal range changes, with implications for future water levels, Scient. Rep., 7, 17021.*

Devlin, A. T., Jay, D. A., Zaron, E. D., Talke, S. A., Pan, J., & Lin, H. (2017, November). Tidal Variability Related to Sea Level Variability in the Pacific Ocean. *Journal of*

Geophysical Research – Oceans, *122*(11), 8445–8463.

Grayver, A. V., & Olsen, N. (2019). The Magnetic Signatures of the M-2, N-2, and O-1 Oceanic Tides Observed in Swarm and CHAMP Satellite Magnetic Data. *Geophysical Research Letters*, *46*(8), 4230–4238.

Haigh, I. D., Pickering, M. D., Green, J. A. M., Arbic, B. K., Arns, A., Dangendorf, S., ... Woodworth, P. L. (2020, March). The Tides They Are A-Changin': A Comprehensive Review of Past and Future Nonastronomical Changes in Tides, Their Driving Mechanisms, and Future Implications. *Reviews of Geophysics*, *58*(1), 1–39.

Love, J. J., & Rigler, E. J. (2014, May). The magnetic tides of Honolulu. *Geophysical Journal International*, *197*(3), 1335–1353.

Mitchum, G. T., & Chiswell, S. M. (2000, December). Coherence of internal tide modulations along the Hawaiian Ridge. *Journal of Geophysical Research – Oceans*, *105*(C), 28–.

Müller, M., Arbic, B. K., & Mitrovica, J. X. (2011, May). Secular trends in ocean tides: Observations and model results. *Journal of Geophysical Research*, *116*(C5).

Ray, R. D. (2006, March). Secular changes of the M tide in the Gulf of Maine. *Continental Shelf Research*, *26*(3), 422–427.

Ray, R. D. (2009, October). Secular changes in the solar semidiurnal tide of the western North Atlantic Ocean. *Geophysical Research Letters*, *36*(19).

Ray, R. D., & Talke, S. A. (2019, October). Nineteenth-Century Tides in the Gulf of Maine and Implications for Secular Trends. *Journal of Geophysical Research – Oceans*, *124*(10), 7046–7067.

Reagan, J. R., Zweng, M. M., Boyer, T. P., Locarnini, R. A., Mishonov, A. V., Baranova, O. K., ... Tyler, R. H. (2020, October). *NOAA Atlas NESDIS 86 WORLD OCEAN ATLAS 2018 Volume 6: Conductivity* (Tech. Rep.).

Sabaka, T. J., Olsen, N., Tyler, R. H., & Kuvshinov, A. (2015). CM5, a pre-Swarm comprehensive geomagnetic field model derived from over 12 yr of CHAMP, Orsted, SAC-C and observatory data. *Geophysical Journal International*, *200*(3), 1596–1626.

Sabaka, T. J., Tøffner-Clausen, L., Olsen, N., & Finlay, C. C. (2018, August). A comprehensive model of Earth's magnetic field determined from 4 years of Swarm satellite observations. *Earth, Planets and Space*, *70*(1), 1531.

Sabaka, T. J., Tøffner-Clausen, L., Olsen, N., & Finlay, C. C. (2020, June). CM6: a comprehensive geomagnetic field model derived from both CHAMP and Swarm satellite observations. *Earth, Planets and Space*, 1–24.

Sabaka, T. J., Tyler, R. H., & Olsen, N. (2016). Extracting ocean-generated tidal magnetic signals from Swarm data through satellite gradiometry. *Geophysical Research Letters*, *43*(7), 3237–3245.

Schnepf, N. R., Nair, M., Maute, A., Pedatella, N. M., Kuvshinov, A., & Richmond, A. D. (2018, August). A Comparison of Model-Based Ionospheric and Ocean Tidal Magnetic Signals With Observatory Data. *Geophysical Research Letters*, *45*(15), 7257–7267.

Sciremammano, F. J. (1979). A suggestion for the presentation of correlations and their significance levels. *Journal of Physical Oceanography*, *9*, 1273–1275.

Talke, S. A., & Jay, D. A. (2020, January). Changing Tides: The Role of Natural and Anthropogenic Factors. *Annual Review of Marine Science*, *12*(1), 121–151.

Tyler, R. H., Maus, S., & Lühr, H. (2003). Satellite Observations of Magnetic Fields Due to Ocean Tidal Flow. *Science*, *299*(5604), 239–241.

Zhao, Z. (2016, September). Internal tide oceanic tomography. *Geophysical Research Letters*, *43*(1), 9157–9164.

Zhao, Z., Alford, M. H., Girton, J., Johnston, T. M. S., & Carter, G. (2011, December). Internal tides around the Hawaiian Ridge estimated from multisatellite altimetry. *Journal of Geophysical Research – Oceans*, *116*(C), C12039.